

## INTER- AND INTRAMOLECULAR LIGAND EXCHANGE REACTIONS OF RUTHENIUM(II) CARBONYL PORPHINE COMPLEXES WITH NITROGEN BASES

S. S. EATON, G. R. EATON and R. H. HOLM

Department of Chemistry, Massachusetts Institute of Technology, Cambridge, Massachusetts 02139 (U.S.A.)

(Received December 23rd, 1971)

### SUMMARY

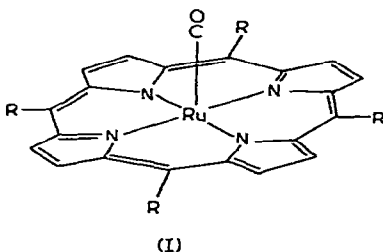
To investigate both inter- and intramolecular site exchange in coordinated nitrogenous bases the complexes of tetra(*p*-isopropylphenyl)porphinato ruthenium carbonyl with 4-*tert*-butylpyridine, 2-methylpyridine, 3,5-dimethylpyrazole, 4,5-dimethylpyridazine, and 3,6-dimethylpyridazine have been studied by total line shape analysis of the variable temperature PMR spectra. Both types of exchange mechanisms have been found in these complexes. All of the complexes undergo intermolecular ligand exchange at rates ranging from  $\sim 0.09 \text{ sec}^{-1}$  ( $\Delta G^\ddagger \sim 19 \text{ kcal/mol}$ ) to  $2 \times 10^4 \text{ sec}^{-1}$  ( $\Delta G^\ddagger \sim 12 \text{ kcal/mol}$ ) at  $25^\circ$  for the various complexes, independent of the concentration of excess ligand. Thus the rate determining step is dissociation. The two pyridazine complexes provide the first examples of intramolecular ligand exchange with coordinated nitrogenous bases. The rates at  $25^\circ$  for intramolecular site exchange ( $\sim 10^6$  and  $66 \text{ sec}^{-1}$ ) are 20–85 times faster than the rates for intermolecular ligand exchange in the same complexes. Within experimental uncertainty there is no intramolecular ligand site exchange in the 3,5-dimethylpyrazole complex. Full kinetic and mechanistic details are discussed.

### INTRODUCTION

Perhaps the most characteristic feature of the chemistry of ruthenium(II) complexes is their non-lability, as evidenced, for example, by the slow rates of substitution of ammine complexes<sup>1</sup> and the retention of enantiomeric<sup>2</sup> and geometrical<sup>3</sup> configurations in the redox cycle  $\text{Ru}^{\text{II}} \rightarrow \text{Ru}^{\text{III}} \rightarrow \text{Ru}^{\text{II}}$  of chelate complexes. Therefore, considerable interest attends the recent report<sup>4</sup> that line broadening in the temperature dependent PMR spectra of  $\text{Ru}(\text{CO})(\text{TPP})^*$  and  $\text{Ru}(\text{CO})(\text{mesoporphyrin}(\text{IX})\text{-dimethyl ester})$  complexes with imidazole and 3,5-dimethylimidazole was due to intramolecular "shuttling" between nitrogen sites of the base and did not involve

\* The following abbreviations are used: TPP, tetraphenylporphinate dianion; *i*-Pr-TPP, tetrakis(*p*-isopropylphenyl)porphinate dianion; *t*-Bupy, 4-*tert*-butylpyridine; 4,4'-Bipy, 4,4'-bipyridyl;  $\alpha$ -Pic,  $\alpha$ -picoline; 3,5-DMP, 3,5-dimethylpyrazole; 3,6-DMPD, 3,6-dimethylpyridazine; 4,5-DMPD, 4,5-dimethylpyridazine;  $\text{DH}^-$ , dimethylglyoximate anion.

intermolecular exchange. Subsequent work<sup>5</sup> in this laboratory revealed that the analogous complex  $\text{Ru}(\text{CO})(i\text{-Pr-TPP})(t\text{-Bupy})$  undergoes intermolecular ligand exchange on the PMR time scale. Independently, Faller and Sibert<sup>6</sup> repeated the measurements of Tsutsui, *et al.*<sup>4a</sup> and demonstrated that within experimental uncertainty the ligand exchange process is entirely intermolecular, with no evidence for a shuttling exchange. Reported in this paper are the results of a total line shape analysis of the temperature dependent PMR spectra of complexes of  $\text{Ru}(\text{CO})(i\text{-Pr-TPP})$  [(I),  $\text{R} = p\text{-isopropylphenyl}$ ] with 3,5-dimethylpyrazole, 3,6-dimethylpyridazine, 4,5-dimethylpyridazine, and  $\alpha$ -picoline. This work provides clearcut examples of both intermolecular ligand exchange and intraligand site exchange.



## EXPERIMENTAL

### Preparation of compounds

Commercial samples of  $\alpha$ -picoline and 3,5-dimethylpyrazole were purified by distillation from barium oxide under nitrogen and by sublimation, respectively. 4,5-Dimethylpyridazine was prepared by published methods<sup>7,8</sup> and was purified by five recrystallizations from petroleum ether containing a small amount of chloroform, followed by drying in vacuum over  $\text{P}_2\text{O}_5$ . 3,6-Dimethylpyridazine was prepared as reported<sup>9</sup> and was purified by repeated fractional distillation followed by partial crystallization of the distillate and, finally, several recrystallizations from cold *n*-hexane. All operations were carried out under nitrogen. The preparation of new compounds is described below; none exhibited a melting point below  $360^\circ$  (sealed tube, in vacuum).

### Tetrakis(*p*-isopropylphenyl)porphine, $\text{H}_2$ (*i*-Pr-TPP)

Starting with *p*-isopropylbenzaldehyde this compound was prepared by a method analogous to that reported for tetraphenylporphine<sup>10</sup>. The crude product was purified by chromatography on Alcoa activated alumina using benzene and trichloroethylene as eluting solvents. The pure compound was obtained as purple crystals. PMR (1,1,2,2-tetrachloroethane, TMS reference) pyrrole protons,  $-8.88$ ; phenyl protons,  $-7.26$  (doublet of doublets, apparent splittings 0.55 and 0.072 ppm); methine,  $-3.23$  (multiplet); methyl,  $-1.53$  (doublet,  $J$  7 Hz); N-H,  $+2.81$  ppm (disappeared upon addition of  $\text{D}_2\text{O}$ ). (Negative shifts are downfield of the reference).

### Tetrakis(*p*-isopropylphenyl)porphinatoruthenium(II) carbonyl, $\text{Ru}(\text{CO})(i\text{-Pr-TPP})$

This compound was obtained by methods similar to those for  $\text{Ru}(\text{CO})(\text{TPP})^4$  and was recrystallized from THF/hexane. This material was further purified by chro-

matography on Woelm neutral alumina. Batches of 50–100 mg dissolved in chloroform were placed on a 4 × 40 cm column and eluted with chloroform. The initial blue eluate contained the free porphyrin. A second band (orange) was eluted. After volume reduction to ca. 1 ml the product crystallized and was collected by filtration. After washing with hexane and drying *in vacuo* at 60° the pure complex was obtained as red crystals.  $\nu(\text{CO})$  1945  $\text{cm}^{-1}$ .

**[(TPP)(CO)Ru]-4,4'-Bipy-[Ru(CO)(TPP)]\***

To a solution of 47.6 mg (0.064 mmol) of Ru(CO)(TPP) in 100 ml of trichloroethylene was added 5.1 mg (0.033 mmol) of 4,4'-bipyridine dissolved in 1 ml of benzene. The solution became more intensely red. After volume reduction to ca. 15 ml a red solid separated, which was filtered and washed with ether yielding 38 mg (72%) of product. (Found: C, 73.20; H, 4.12; N, 8.58.  $\text{C}_{100}\text{H}_{64}\text{N}_{10}\text{O}_2\text{Ru}_2$  calcd.: C, 73.25; H, 3.93; N, 8.54%)  $\nu(\text{CO})$  1968  $\text{cm}^{-1}$ .

**Ru(CO)(TPP)(*t*-Bupy)**

To 50 mg (0.067 mmol) of Ru(CO)(TPP) dissolved in 50 ml of trichloroethylene was added 9 mg (0.07 mmol) of 4-*tert*-butylpyridine. A darker red color developed. The volume was reduced to 15 ml and 25 ml of hexane were slowly added. The red-violet crystals which formed upon standing were filtered and washed with hexane, yielding 40 mg (68%) of product. (Found: C, 73.52; H, 4.88; N, 8.01.  $\text{C}_{53}\text{H}_{43}\text{N}_5\text{ORu}$  calcd.: C, 73.42; H, 5.00; N, 8.08%)  $\nu(\text{CO})$  1965  $\text{cm}^{-1}$ .

**Ru(CO)(*i*-Pr-TPP)(*t*-Bupy)**

A solution of 100 mg (0.11 mmol) of Ru(CO)(*i*-Pr-TPP) and 15 mg (0.11 mmol) of 4-*tert*-butylpyridine in 10 ml of trichloroethylene was filtered and reduced in volume to ca. 3 ml. Addition of ca. 7 ml of hexane caused crystals to separate. These were recrystallized twice from trichloroethylene/hexane containing excess 4-*tert*-butylpyridine, yielding 99 mg (85%) of red-violet crystals. (Found: C, 75.71; H, 6.34; N, 6.87.  $\text{C}_{66}\text{H}_{65}\text{N}_5\text{ORu}$  calcd.: C, 75.83; H, 6.27; N, 6.70%)  $\nu(\text{CO})$  1955  $\text{cm}^{-1}$ .

**Ru(CO)(*i*-Pr-TPP)(3,5-DMP)**

Addition of 22 mg (0.23 mmol) of 3,5-dimethylpyrazole to a slurry of 102 mg (0.11 mmol) of Ru(CO)(*i*-Pr-TPP) in 3 ml of trichloroethylene produced a clear red solution. Reduction of the volume to ca. 1 ml and slow addition of hexane precipitated violet crystals. These were recrystallized from trichloroethylene/hexane containing excess 3,5-dimethylpyrazole, affording 90 mg (80%) of violet crystals. (Found: C, 73.80; H, 6.16; N, 8.42.  $\text{C}_{62}\text{H}_{60}\text{N}_6\text{ORu}$  calcd.: C, 74.00; H, 6.01; N, 8.35%)  $\nu(\text{CO})$  1958  $\text{cm}^{-1}$ .

**Infrared spectra**

Spectra were recorded as Kel-F mulls using a Perkin-Elmer 337 grating spectrometer. The observation of a single sharp carbonyl absorption in the infrared spectra is consistent with the structure (I).

\* This compound was erroneously reported as the *p*-isopropyl derivative in ref. 5.

### PMR spectra

Spectra were obtained using a Varian HA-100 spectrometer equipped with a variable temperature probe and operated at power levels well below saturation. Temperatures were measured with a thermocouple mounted in the probe which was calibrated with methanol and ethylene glycol after each set of spectra. Reagent grade trichloroethylene ( $C_2HCl_3$ ) was degassed by several freeze-thaw cycles and stored under nitrogen. 1,1,2-Tetrachloroethane ( $C_2H_2Cl_4$ ) was purified by distillation from  $P_2O_5$  under nitrogen. Solutions for PMR study were prepared under nitrogen immediately before use, but there was no evidence of decomposition in samples which were kept at room temperature for several weeks. A small amount of decomposition was noted, however, in samples which were heated above the boiling point of the solvent. Spectra were obtained with the spectrometer locked on the solvent resonance. 60 Hz sidebands on the isopropyl doublet evident in some of the spectra are due to electronic pickup in the spectrometer.

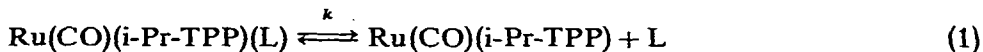
### Kinetic analysis

The kinetics of the inter- and intramolecular ligand exchange processes were determined by visual comparison of calculated and observed temperature dependent line shapes of methyl PMR signals. The narrowest scan widths (usually 50 or 100 Hz) consistent with the spectral line widths were used in the comparison of calculated and observed spectra. Spectra with larger scan widths are presented in the figures for the purpose of clarity. Simulated spectra were calculated by total line shape analysis using a modification<sup>11</sup> of the Whitesides-Lisle EXCNMR computer program<sup>12</sup>. The use of this program has been discussed in detail elsewhere<sup>13</sup>. The dynamic processes were treated as simple two-site exchanges in the case of t-Bupy and  $\alpha$ -Pic, and as three-site exchanges in the case of 3,5-DMP, 3,6-DMPD, and 4,5-DMPD. The non-exchange line widths were interpolated between the observed slow-exchange and fast-exchange widths, with the aid of separate measurements of the line width in solutions of the ligand without complex present. Non-exchange chemical shift extrapolations were based on the curvatures of the slow-exchange shifts, adjusted to fit the observed fast-exchange average shift.  $\tau$  (sec) is defined as the mean pre-exchange lifetime of a methyl group in a given coordination environment. Thus,  $k=1/\tau$  is the exchange rate in  $sec^{-1}$  for exchange between a coordinated site and either free ligand or another coordinated site, as specified in each case. Activation parameters were determined from weighted least squares Arrhenius ( $\ln 1/\tau$  vs.  $1/T$ ) and Eyring ( $\ln h/k \cdot T \cdot \tau$  vs.  $1/T$ ) plots.

In the following sections the temperature dependent spectra and chemical shifts shown in Figs. 1-7 for individual systems containing  $Ru(CO)(i-Pr-TPP)$  and free base are considered. Arrhenius plots of the kinetic data are in Fig. 8.  $Ru(CO)(i-Pr-TPP)$  rather than  $Ru(CO)(TPP)$  was employed because its solubility is about ten times larger in the solvents suitable for PMR studies. The isopropyl doublet occurs in all of the spectra (Figs. 1, 2, 4, and 6).

In each complex the coordinated ligand peaks are shifted to higher field than the free ligand peaks. The large magnitude of the shifts (0.93 to 4.47 ppm) caused by the diamagnetic anisotropy of the porphyrin complex<sup>14</sup> results in a large temperature range over which the exchange processes can be studied, and hence makes it possible to get accurate kinetic parameters. Two different exchange processes were

observed. The intermolecular exchange shown in eqn. (1) was observed in all of the complexes. In addition, in the pyridazine complexes the intramolecular ligand site exchange shown in eqn. (2) was observed.



#### *Ru(CO)(i-Pr-TPP)(t-Bupy)*

The preformed crystalline complex and excess *t*-Bupy were dissolved in  $\text{C}_2\text{H}_2\text{-Cl}_4$  under nitrogen. At  $25^\circ$  the PMR signal for the tert-butyl group of coordinated *t*-Bupy was shifted 0.93 ppm to higher field than the tert-butyl group in free *t*-Bupy present in equimolar excess (0.085 *M* in each component). As the temperature was increased both peaks broadened, moved together, and coalesced to a single sharp peak at the average of the extrapolated positions of the separate peaks as is typical of two-site exchange reactions. (The spectra have been shown previously<sup>5</sup>.) Dilution of the total concentration by factors of two and four produced no change in the line-shape as a function of temperature, indicating a first-order process. The exchange process involved is given in eqn. (1). Lineshape analysis using a constant ratio of free to coordinated *t*-Bupy yielded linear Eyring and Arrhenius plots and the kinetic parameters given in Table 1 and Fig. 8.

#### *Ru(CO)(i-Pr-TPP)(\alpha-Pic)* (cf. Fig. 1)

Samples for NMR study were prepared by dissolving  $\text{Ru(CO)(i-Pr-TPP)}$  in 1/3 v/v  $\text{C}_2\text{H}_2\text{Cl}_4/\text{C}_2\text{HCl}_3$  in the presence of excess  $\alpha\text{-Pic}$ . Over the temperature range  $-60^\circ$  to  $-20^\circ$  the methyl PMR signal for the coordinated  $\alpha\text{-Pic}$  was observed ca. 3.9 ppm to higher field than the methyl signal for free  $\alpha\text{-Pic}$ . As the temperature was

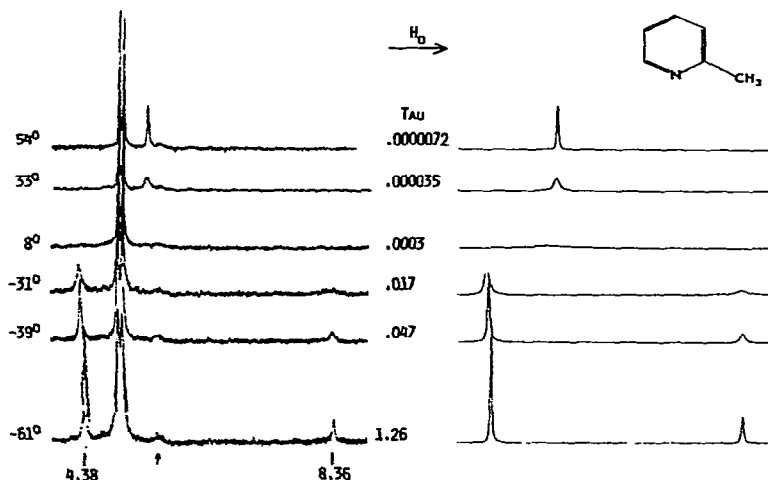


Fig. 1. 100 MHz methyl PMR spectra of a mixture of  $\text{Ru(CO)(i-Pr-TPP)}$  (0.034 *M*) and  $\alpha\text{-Pic}$  (0.097 *M*) in 1/3 v/v  $\text{C}_2\text{H}_2\text{Cl}_4/\text{C}_2\text{HCl}_3$  at various temperatures compared with spectra calculated by line shape analysis. The arrow marks an impurity. Slow exchange chemical shifts are in ppm upfield of the  $\text{C}_2\text{H}_2\text{Cl}_4$  lock signal.  $\tau$  Values are in seconds.

increased the signals broadened and coalesced to a single peak. Since a small impurity peak was noticed, the measurements were repeated using redistilled  $\alpha$ -Pic. Similar results were obtained from both measurements. Because Ru(CO)(i-Pr-TPP)( $\alpha$ -Pic) is substantially dissociated under the conditions of the measurement, the ratio of free to coordinated  $\alpha$ -Pic assumed in the lineshape analysis must be obtained from the peak areas in the slow-exchange spectra and the shift of the coalesced peak, rather than from the way the sample was prepared. Within the uncertainty of these methods of estimating population ratios, about  $0.8 \pm 0.1$  of the Ru(CO)(i-Pr-TPP) was coordinated by  $\alpha$ -Pic under the conditions of the NMR measurements. Consequently, calculated spectra for comparison with the observed spectra were generated for a range of population ratios for each sample. The resulting kinetic parameters did not depend strongly on the assumed population ratio due to the large chemical shift difference between the free and coordinated methyl resonances and the large temperature range over which the samples were studied ( $-61^\circ$  to  $+72^\circ$ ). Average parameters for the  $\alpha$ -Pic system with error limits which reflect the uncertainty in the above analysis are listed in Table 1.  $\tau$  Values are given in Fig. 8.

TABLE 1

KINETIC PARAMETERS<sup>a</sup> FOR INTERMOLECULAR (HTP) AND INTRAMOLECULAR (LTP) LIGAND EXCHANGE OF Ru(CO)(i-Pr-TPP) (L) COMPLEXES

L	Conc. (M)		$\Delta G_{298}^\ddagger$ (kcal/mol)	$\Delta H^\ddagger$ (kcal/mol)	$\Delta S^\ddagger$ (eu)	$E_a$ (kcal/mol)	log A	$k_{298}$ (sec <sup>-1</sup> )	$T_c^b$ (°C)
	L	Ru <sup>II</sup>							
t-Bupy <sup>c</sup>	0.18	0.086	18.9 ± 2.5	20.6 ± 2.0	5.6 ± 5.1	21.3 ± 2.0	14.6 ± 1.1	0.09 <sup>h</sup>	106
$\alpha$ -Pic <sup>d,f</sup>	0.097	0.034	11.7 ± 1.3	13.9 ± 0.4	7.1 ± 1.7	14.4 ± 0.4	14.8 ± 0.7	1.6 × 10 <sup>4</sup>	-2
3,5-DMP <sup>c,g</sup>	0.11	0.11	16.9 ± 1.4	17.6 ± 1.1	2.3 ± 3.0	18.3 ± 1.1	13.8 ± 0.6	2.5 <sup>h</sup>	100
3,5-DMP <sup>c</sup>	0.24	0.12	16.9 ± 2.0	18.4 ± 1.6	4.8 ± 4.1	19.1 ± 1.6	14.4 ± 0.9	2.4 <sup>h</sup>	95
3,5-DMP <sup>c</sup>	0.30	0.093	16.9 ± 2.1	18.2 ± 1.6	4.4 ± 4.6	19.0 ± 1.0	14.3 ± 1.0	2.6 <sup>h</sup>	97
4,5-DMPD									
HTP <sup>c</sup>	0.19	0.049	16.6 ± 1.0	17.4 ± 0.8	2.6 ± 2.2	18.1 ± 0.8	13.9 ± 0.5	4.2 <sup>h</sup>	83
HTP <sup>c</sup>	0.11	0.055	16.9 ± 3.4	18.8 ± 2.5	6.6 ± 7.7	19.5 ± 2.5	14.7 ± 1.7	2.9 <sup>h</sup>	
LTP <sup>c</sup>	0.19	0.049	14.7 ± 2.1	13.5 ± 1.5	-4.1 ± 5.1	14.0 ± 1.5	12.3 ± 1.1	105	22
LTP <sup>c</sup>	0.11	0.055	15.1 ± 1.8	15.1 ± 1.3	0.0 ± 4.4	15.6 ± 1.3	13.2 ± 1.0	66	28
3,6-DMPD <sup>c</sup>									
HTP <sup>c</sup>	0.12	0.052	11.8 ± 1.2	13.6 ± 0.8	5.9 ± 2.9	14.2 ± 0.8	14.5 ± 0.6	1.3 × 10 <sup>4</sup>	-2
LTP <sup>c</sup>	0.12	0.052	9.4 ± 2.0	12.1 ± 1.2	9.2 ± 5.2	12.6 ± 1.2	15.1 ± 1.1	1.1 × 10 <sup>6h</sup>	~ -50

<sup>a</sup> Error limits given are three times the standard deviations in least squares fits to the Eyring or Arrhenius equations.

<sup>b</sup> Coalescence temperature. <sup>c</sup> C<sub>2</sub>H<sub>2</sub>Cl<sub>4</sub> solution. <sup>d</sup> 1/3 v/v C<sub>2</sub>H<sub>2</sub>Cl<sub>4</sub>/C<sub>2</sub>HCl<sub>3</sub> solution. <sup>e</sup> 1/2 v/v C<sub>2</sub>H<sub>2</sub>Cl<sub>4</sub>/C<sub>2</sub>HCl<sub>3</sub> solution.

<sup>f</sup> Values given are the average of four calculations; two different extrapolations for each of two samples of nearly the same concentration (see text). <sup>g</sup> Values given were calculated using  $\tau$  values equal to one-half the  $\tau$  values which gave agreement of calculated and observed spectra. The best-fit  $\tau$  values yield  $\Delta S^\ddagger$   $0.9 \pm 3.0$  eu, log A  $13.5 \pm 1.5$ , and  $k_{298}$   $1.2 \text{ sec}^{-1}$ . <sup>h</sup> Extrapolated values.

### Ru(CO)(i-Pr-TPP)(3,5-DMP) (cf. Fig. 2 and 3)

The variable temperature PMR spectra of C<sub>2</sub>H<sub>2</sub>Cl<sub>4</sub> solutions of Ru(CO)(i-Pr-TPP)(3,5-DMP) were studied as a function of concentration of excess 3,5-DMP and of total concentration of the sample. At 29° the methyl resonances of the coordinated 3,5-DMP were shifted 1.50 ppm and 3.97 ppm to higher field than the methyl

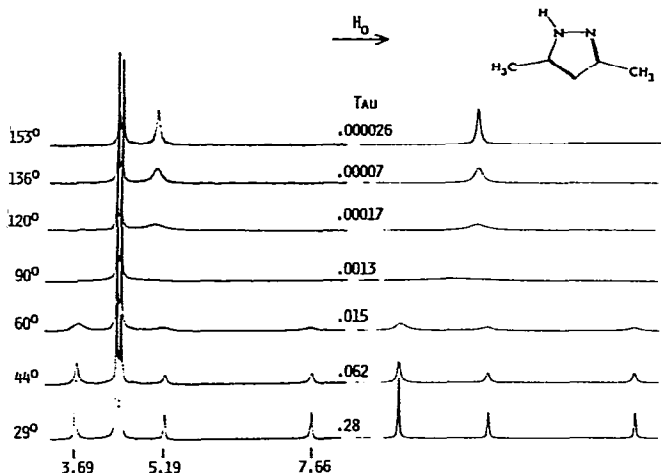


Fig. 2. 100 MHz methyl PMR spectra of a 1/1 mixture of Ru(CO)(i-Pr-TPP)(3,5-DMP) (0.12 M) and 3,5-DMP (0.12 M) in  $C_2H_2Cl_4$  at various temperatures compared with spectra calculated by line shape analysis. Slow exchange chemical shifts are in ppm upfield of the  $C_2H_2Cl_4$  lock signal.  $\tau$  Values are in seconds.

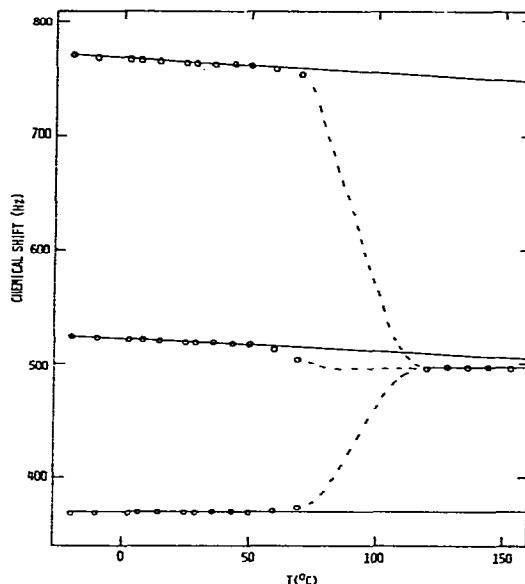
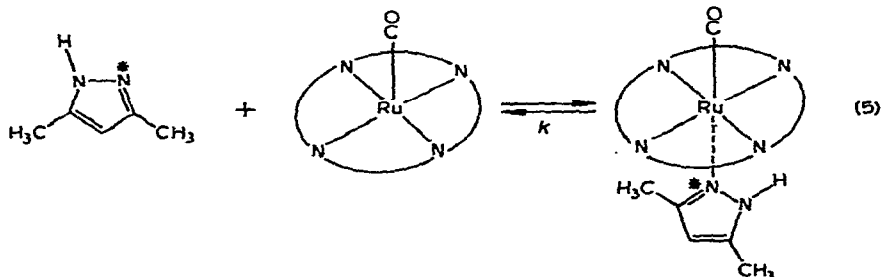
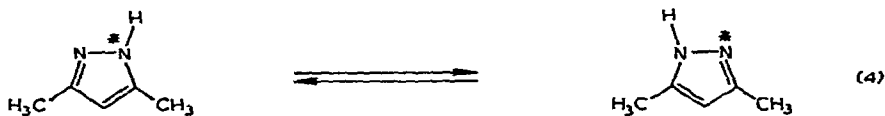
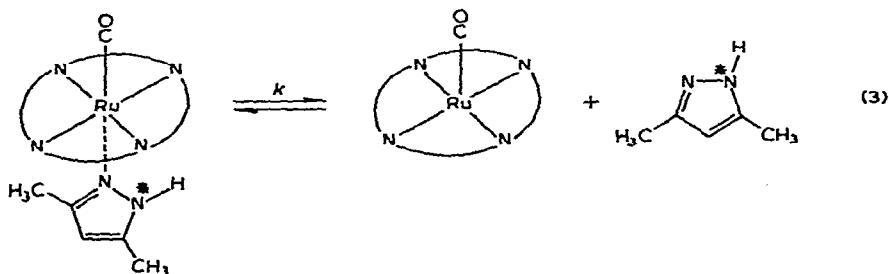


Fig. 3. Temperature dependence of the 3,5-DMP methyl chemical shifts in a 1/1 mixture of Ru(CO)(i-Pr-TPP)(3,5-DMP) (0.12 M) and 3,5-DMP (0.12 M) in  $C_2H_2Cl_4$ . The shifts are plotted in Hz upfield of the  $C_2H_2Cl_4$  lock signal. The low-field resonance due to free 3,5-DMP and the two high-field resonances of coordinated 3,5-DMP simultaneously coalesce to a single resonance. The solid lines indicate the chemical shift extrapolations used in the line shape analysis.

resonances of free 3,5-DMP present in the solution. In free 3,5-DMP the methyl groups are equivalent since the compound forms hydrogen-bonded dimers and trimers in solution<sup>15</sup>. A sample prepared by dissolving preformed Ru(CO)(i-Pr-TPP)(3,5-DMP) in  $C_2H_2Cl_4$  exhibited two peaks of equal area due to coordinated 3,5-DMP which broadened and moved together and coalesced above 100° to a single peak at the average of the extrapolated positions of the separate peaks. No free 3,5-DMP was observed in this sample. A second sample, in which Ru(CO)(i-Pr-TPP)(3,5-DMP) and excess 3,5-DMP were dissolved in a 1/1 ratio in  $C_2H_2Cl_4$  exhibited three methyl resonances of relative intensity 2/1/1 which simultaneously broadened and coalesced to a single peak in the same temperature range (Fig. 2). In this case the coalesced peak occurred at the weighted average of the extrapolated shifts of the three separate peaks (Fig. 3). In the lineshape analysis attempts were made to simulate the observed spectra assuming both an intramolecular exchange process and an intermolecular exchange process. The observed spectra are incompatible with an intramolecular exchange between ligand sites proceeding at a rate greater than 10% of the intermolecular exchange rate (limit of experimental accuracy). Variable temperature PMR studies of the same sample, diluted by factors of two and four, produced no difference in the lineshape as a function of temperature. A third sample, with a 2.2/1 ratio of Ru(CO)(i-Pr-TPP)(3,5-DMP) to 3,5-DMP, yielded similar results.

For all three samples lineshape analysis using a constant ratio of free to coordinated 3,5-DMP yielded linear Eyring and Arrhenius plots. For the sample without excess 3,5-DMP the kinetic process observed is exchange between coordinated methyl groups. In the samples containing excess 3,5-DMP the kinetic process observed is exchange between free and coordinated methyl groups. In each case it is assumed that proton exchange from one nitrogen to the other occurs rapidly while the 3,5-DMP is not coordinated. With no excess 3,5-DMP present only half of the actual dissociations effect methyl exchange, so in this case the  $\tau$  values were divided by two, affording kinetic parameters (*cf.* Table 1 and Fig. 8) for all samples which refer to a dissociative process as depicted in eqns. (3)–(5).



The good agreement between the kinetic parameters obtained for the three samples substantiates the assumption that dissociation [eqn. (3)] is the rate-determining step and that exchange between ligand binding sites occurs by an intermolecular route.

#### *Ru(CO)(i-Pr-TPP)(4,5-DMPD)* (*cf.* Fig. 4 and 5)

PMR studies were made of  $Ru(CO)(i-Pr-TPP)$  and excess 4,5-DMPD dissolved in  $C_2H_2Cl_4$  and 1/2 v/v  $C_2H_2Cl_4/C_2HCl_3$ . In both cases the  $Ru(CO)(i-Pr-TPP)$  appeared to be fully coordinated by the 4,5-DMPD over the entire temperature range studied. Below  $\sim 12^\circ$  the methyl resonances of the coordinated 4,5-DMPD were observable as separate peaks shifted 1.22 and 1.51 ppm to higher field than the methyl resonance of free 4,5-DMPD present in the solution. As the temperature was increased



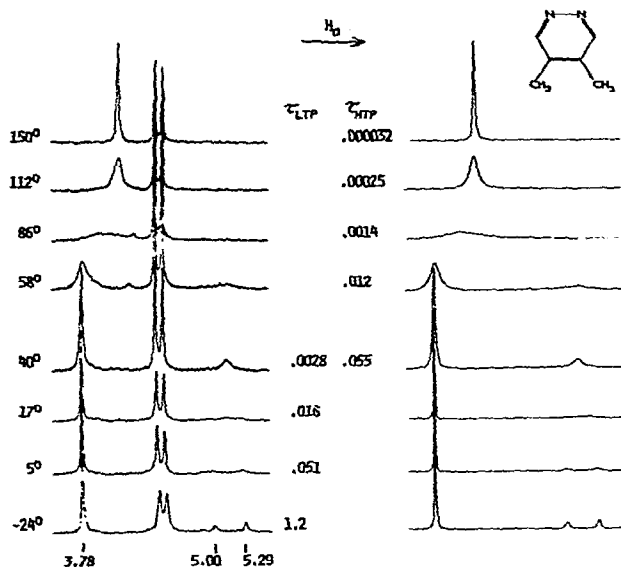


Fig. 4. 100 MHz methyl PMR spectra of a mixture of  $\text{Ru}(\text{CO})(i\text{-Pr-TPP})$  (0.049 M) and 4,5-DMPD (0.19 M) in  $\text{C}_2\text{H}_2\text{Cl}_4$  at various temperatures compared with spectra calculated by line shape analysis. Slow exchange chemical shifts are in ppm upfield of the  $\text{C}_2\text{H}_2\text{Cl}_4$  lock signal.  $\tau$  Values are in seconds.

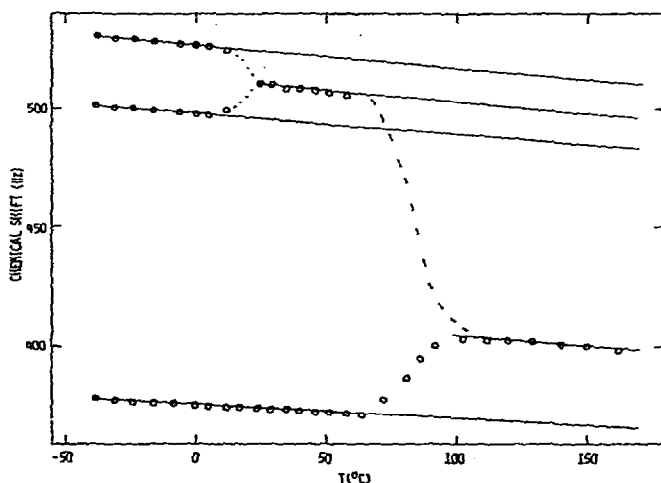
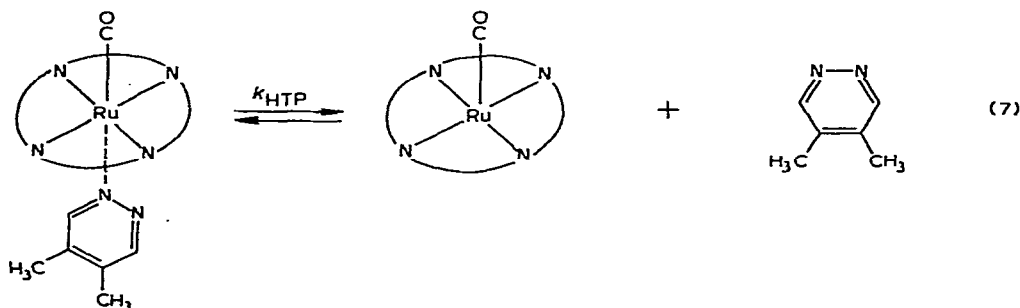
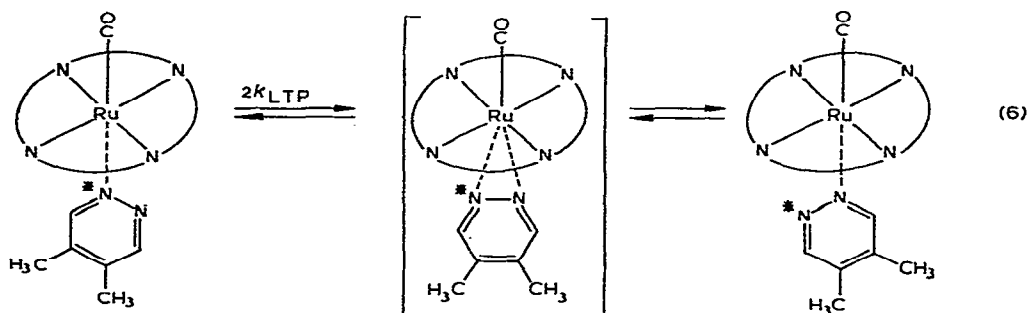


Fig. 5. Temperature dependence of the 4,5-DMPD methyl chemical shifts in a mixture of  $\text{Ru}(\text{CO})(i\text{-Pr-TPP})$  (0.049 M) and 4,5-DMPD (0.19 M) in  $\text{C}_2\text{H}_2\text{Cl}_4$ . The shifts are plotted in Hz upfield of the  $\text{C}_2\text{H}_2\text{Cl}_4$  lock signal. The two high-field resonances due to coordinated 4,5-DMPD coalesce to a single peak which then coalesces with the low-field free 4,5-DMPD peak yielding a single resonance. The solid lines indicate the chemical shift extrapolations used in the line shape analysis.

the coordinated methyl resonances broadened, moved together, and coalesced to a single peak which reached minimum linewidth at  $\sim 40^\circ$  and then broadened again and coalesced with the methyl resonance of the free 4,5-DMPD at the weighted average of the extrapolated shifts (Fig. 4 and 5). Since the increased viscosity of

$C_2H_2Cl_4$  below room temperature causes significant broadening of the spectra and thus additional uncertainty in the nonexchange linewidth, a sample was studied using the less viscous 1/2 v/v mixture of  $C_2H_2Cl_4/C_2HCl_3$ . Although this solvent mixture permitted more extensive low temperature study, the low boiling point of  $C_2HCl_3$  precluded study above the coalescence temperature for the high temperature process. Consequently, the kinetic parameters given in Table 1 and Fig. 8 for the low temperature process are more accurate for the sample dissolved in the  $C_2H_2Cl_4/C_2HCl_3$  mixture and for the high temperature process are more accurate for the sample dissolved in  $C_2H_2Cl_4$ . In addition there is a solvent effect on the low temperature process, the rate in  $C_2H_2Cl_4$  being about twice the rate in  $C_2H_2Cl_4/C_2HCl_3$ . In performing the lineshape analysis a constant ratio of free to coordinated 4,5-DMPD was used consistent with peak areas and shift extrapolations, and linear Eyring and Arrhenius plots were obtained. The sequence of lineshape changes compels interpretation in terms of two processes, the low temperature process ( $-24^\circ$  to  $+40^\circ$ ) wholly intramolecular and the high temperature process ( $30^\circ$  to  $150^\circ$ ) intermolecular, as in eqn. (6) and (7). The representation of the intermediate in eqn. (6) is speculative.



#### $Ru(CO)(i-Pr-TPP)(3,6-DMPD)$ (cf. Figs. 6 and 7)

Below  $\sim -70^\circ$  in a sample prepared by dissolving  $Ru(CO)(i-Pr-TPP)$  and excess 3,6-DMPD in 1/2 v/v  $C_2H_2Cl_4/C_2HCl_3$  the methyl resonances of coordinated 3,6-DMPD were shifted 1.33 and 4.47 ppm to higher field than the methyl resonance of free 3,6-DMPD. The lower field coordinated methyl resonance was partially superimposed on the *i*-Pr resonance of  $Ru(CO)(i-Pr-TPP)$ . As the temperature was increased the coordinated methyl resonances coalesced to a single peak which reached minimum linewidth ( $\sim 40$  Hz) at  $\sim -28^\circ$  and then broadened again and coalesced

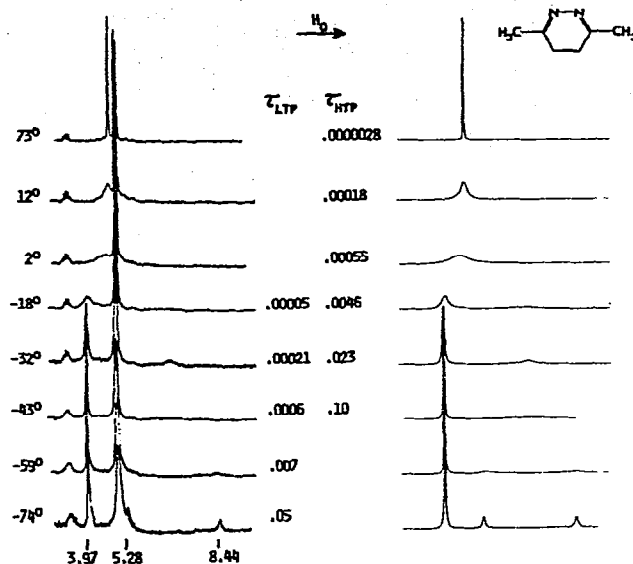


Fig. 6. 100 MHz methyl PMR spectra of a mixture of  $\text{Ru}(\text{CO})(i\text{-Pr-TPP})$  (0.052 M) and 3,6-DMPD (0.12 M) in  $1/2 \text{C}_2\text{H}_2\text{Cl}_4/\text{C}_2\text{HCl}_3$  at various temperatures compared with spectra calculated by line shape analysis. Slow exchange chemical shifts are in ppm upfield of the  $\text{C}_2\text{H}_2\text{Cl}_4$  lock signal.  $\tau$  Values are in seconds.

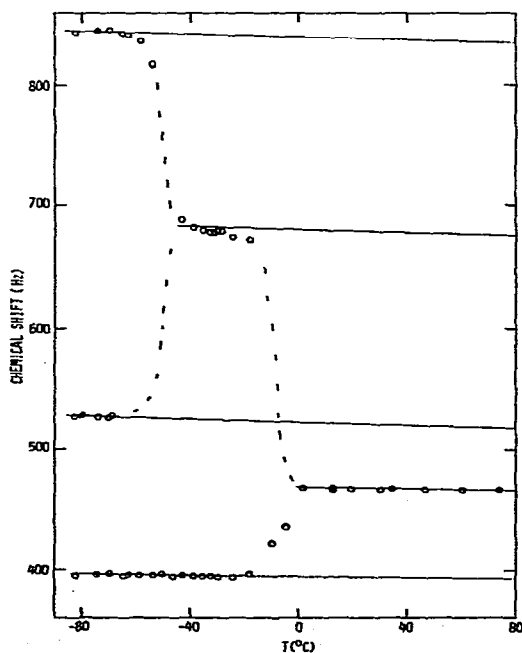


Fig. 7. Temperature dependence of the 3,6-DMPD methyl chemical shifts in a mixture of  $\text{Ru}(\text{CO})(i\text{-Pr-TPP})$  (0.052 M) and 3,6-DMPD (0.12 M) in  $1/2 \text{C}_2\text{H}_2\text{Cl}_4/\text{C}_2\text{HCl}_3$ . The shifts are plotted in Hz upfield of the  $\text{C}_2\text{H}_2\text{Cl}_4$  lock signal. The two high-field resonances due to coordinated 3,6-DMPD coalesce to a single peak which subsequently coalesces with the low-field peak due to free 3,6-DMPD giving a single resonance. The solid lines indicate the chemical shift extrapolations used in the line shape analysis.

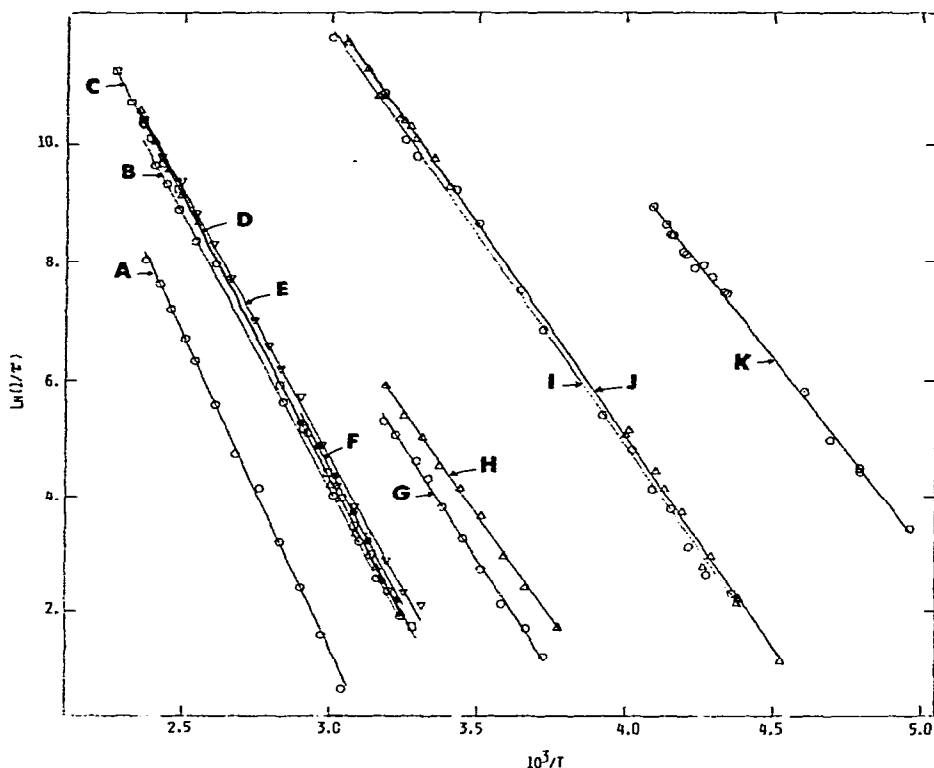


Fig. 8. Arrhenius plots for ligand exchange reactions of complexes of  $\text{Ru}(\text{CO})(i\text{-Pr-TPP})$  with the nitrogenous bases: A. *t*-Bupy, B. equimolar 3,5-DMP, C. 2.2 mole ratio excess 3,5-DMP, D. 1.0 mole ratio excess 3,5-DMP, E. 4,5-DMPD in  $\text{C}_2\text{H}_2\text{Cl}_4$ , F. 4,5-DMPD in  $1/2 \text{C}_2\text{H}_2\text{Cl}_4/\text{C}_2\text{HCl}_3$ , G. 4,5-DMPD in  $1/2 \text{C}_2\text{H}_2\text{Cl}_4/\text{C}_2\text{HCl}_3$  intramolecular process, H. 4,5-DMPD in  $\text{C}_2\text{H}_2\text{Cl}_4$  intramolecular process, I. 3,6-DMPD, J.  $\alpha$ -Pic, K. 3,6-DMPD intramolecular process.

with the methyl resonance of the free 3,6-DMPD at the weighted average of the extrapolated shifts (Fig. 6 and 7).  $\text{Ru}(\text{CO})(i\text{-Pr-TPP})(3,6\text{-DMPD})$  is extensively dissociated under the conditions of the PMR measurements. Best fit between calculated and observed spectra was obtained by increasing the ratio of free to coordinated 3,6-DMPD from 2.2 at  $-69^\circ$  to 2.9 at  $73^\circ$ . Using these population ratios and the chemical shift extrapolations shown in Fig. 7, lineshape analysis yielded linear Eyring and Arrhenius plots and the kinetic parameters given in Table 1 and Fig. 8. In view of the small temperature range in which the coordinated methyl resonances were observed below the coalescence temperature, the kinetic parameters for the low temperature process are less certain than in the case of 4,5-DMPD. However, the linewidth behavior as a function of temperature compels interpretation in terms of an intramolecular low temperature process ( $-74^\circ$  to  $-18^\circ$ ) and an intermolecular high temperature process ( $-43^\circ$  to  $73^\circ$ ) similar to those given in eqn. (6) and (7) for 4,5-DMPD.

## DISCUSSION

Analysis of the temperature dependent methyl PMR spectra of five nitrogen

donor ligands in the presence of  $\text{Ru}(\text{CO})(i\text{-Pr-TPP})$  in weakly polar media has provided evidence for two types of kinetic processes. All of the complexes  $\text{Ru}(\text{CO})(i\text{-Pr-TPP})(\text{L})$  undergo intermolecular ligand exchange [eqn. (1)]. Studies of the effect of concentration of  $\text{Ru}^{\text{II}}$  complex and ligand on exchange rates has provided satisfactory evidence that the slow step in the exchange process is rupture of the  $\text{Ru-N}$  bond. Rates at  $25^\circ$  for this process vary from ca.  $10^{-1}$  to  $10^4 \text{ sec}^{-1}$ , with the faster rates found for pyridine or pyridazine ligands having a methyl group on the carbon adjacent to the donor site. Activation entropies for intermolecular exchange are uniformly small positive quantities (2.3 to 7.1 eu). Complexes of 4,5-DMPD and 3,6-DMPD are clearly involved in two kinetic processes. That occurring at higher temperatures (HTP) is intermolecular exchange whereas the low temperature process (LTP) results from intramolecular site exchange [eqn. (2)] involving the two equivalent donor sites of the ligands.  $\text{Ru}(\text{CO})(i\text{-Pr-TPP})(4,5\text{-DMPD})$  and  $\text{Ru}(\text{CO})(i\text{-Pr-TPP})(3,6\text{-DMPD})$  represent the first authenticated examples of this exchange process with nitrogenous bases. At  $25^\circ$  the rates of intramolecular exchange are ca. 20–85 times faster than intermolecular ligand exchange (Table 1) and are characterized by values of  $\Delta G_{298}^\ddagger$  which are ca. 2 kcal/mol smaller than those for the HTP in the same solvent. Both intermolecular and intramolecular exchange rates are larger for 3,6-DMPD, which contains methyl groups near the donor sites, than for 4,5-DMPD. Crystalline 1/1 adducts were isolated with *t*-Bupy and 3,5-DMP. A binuclear adduct was isolated with 4,4'-Bipy but its low solubility precluded PMR studies of ligand exchange.

#### *Intermolecular ligand exchange*

Ligand exchange of  $\text{Ru}(\text{CO})(i\text{-Pr-TPP})(\text{L})$  species occurs at rates which are in excess of those usually found for substitution reactions of  $\text{Ru}^{\text{II}}$  complexes which involve displacement of a nitrogen-bound ligand. The limited body of kinetic data available refers mainly to aquation reactions of  $[\text{Ru}^{\text{II}}(\text{NH}_3)_5\text{L}]^{+2}$ . When L is a potential  $\pi$ -donor ligand such as formate or trifluoroacetate, it is quite labile and aquation rates of ca.  $1\text{--}600 \text{ sec}^{-1}$  at  $25^\circ$  have been found. However, when L has  $\pi$ -acid properties (e.g., Py,  $\text{N}_2$ ) the complexes undergo substitution reactions very slowly or not at all<sup>1</sup>. The aquation rate of  $\text{Ru}(\text{NH}_3)_6^{+2}$  in acid solution at  $25^\circ$  is  $1.2 \times 10^{-3} \text{ M}^{-1} \cdot \text{sec}^{-1}$ , a factor of ca.  $10^3\text{--}10^4$  times slower than for aquation of pentammine complexes containing oxygen ligands. While these kinetic results are not strictly comparable to the data in Table 1 because of differences in solvent and reaction order, they nonetheless serve to indicate that the exchange reactions reported here occur at rates at least several orders of magnitude greater than previously observed for reactions involving displacement of nitrogen donor ligands bonded to  $\text{Ru}^{\text{II}}$ .

There have been no reports of kinetic studies either on other  $\text{Ru}^{\text{II}}$  complexes or on other metalloporphyrin complexes which permit direct comparison with the results obtained in this investigation. In order to place our observations in perspective, previous work on the formation and lability of metalloporphyrin-base complexes will be considered briefly in the following sections. No direct quantitative comparison with the present results is intended.

A full explanation of the lability observed for  $\text{Ru}(\text{CO})(i\text{-Pr-TPP})(\text{L})$  complexes requires a detailed knowledge of their electronic properties, including both bonded and non-bonded (steric) interactions. In the absence of such information it is still worthwhile to explore the qualitative implications of the rate differences observed.

Because the rate-determining step in intermolecular ligand exchange is dissociation of the ligand, activation energies, particularly activation enthalpies, may be expected to be influenced by steric and electronic properties of the ligands. If the predominant energy term in the dissociation step were related to the metal–ligand bond energy, relative rates might bear a relationship to relative stabilities or heats of formation of complexes formed by these ligands. For certain of the ligands used in this study no correlation of  $\Delta H^\ddagger$  with base strengths, as measured by  $pK_a$  values, is anticipated. Hydrogen-bonded dimer and trimer formation by unprotonated 3,5-DMP<sup>15</sup> lowers its  $pK_a$  and similar dimer formation by protonated pyridazines increases their  $pK_a$  values relative to those expected in the absence of hydrogen-bonding effects<sup>16,17</sup>.

From the data in Table 1 it is observed that at 25° the exchange rate for  $\alpha$ -Pic is ca.  $2 \times 10^5$  times faster than for t-Bupy whereas the intermolecular rates for  $\alpha$ -Pic and 3,6-DMPD are nearly equal as are those for 3,5-DMP and 4,5-DMPD. Evidently, steric factors caused by the position of methyl substitution have a major effect on relative exchange rates. Steric effects are manifest in the relative stabilities of other pyridine complexes. For example, the heat of formation of the complex of 4-Mepy with  $B(CH_3)_3$  is ca. 5.9 kcal/mol greater than that of  $\alpha$ -Pic with the same acceptor<sup>18</sup>. A similar difference is expected between complexes of 4-t-Bupy and  $\alpha$ -Pic. A linear correlation has been observed between the log of the formation constant of  $Zn(TPP)(L)$  complexes and the  $pK_a$  values of 3- and 4-substituted pyridines<sup>19</sup>. However,  $\alpha$ -Pic and 2,4,6-Me<sub>3</sub>Py deviate from the correlation, and the weaker complexes formed by these ligands were attributed to steric effects<sup>19</sup>. Using published data<sup>18–20</sup> a linear relation between heats of formation of  $B(CH_3)_3(L)$  and formation constants of  $M(TPP)(L)$  complexes  $M = Zn^{II}, Cd^{II}, Hg^{II}$  is obtained. An exception is found for the case of  $L = 2,4,6-Me_3Py$  which forms a stronger complex with  $Zn(TPP)$  than might be expected from the correlation. It is noted that the difference in  $\Delta H^\ddagger$  values for t-Bupy and  $\alpha$ -Pic exchange with  $Ru(CO)(i-Pr-TPP)$ ,  $6.7 \pm 2.0$  kcal/mol, is near to the value of ca. 6 kcal/mol anticipated if activation enthalpies are related to metal–ligand bond strengths. While this close agreement obviously cannot be given quantitative significance, it does tend to support the overall impression given by the data in Table 1 and Fig. 8: relative ligand exchange rates are principally controlled by steric effects, modulated by differences in base strengths.

#### *Intramolecular ligand site exchange*

The original claim of an intramolecular kinetic process involving nitrogen donor ligands was put forward by Tsutsui *et al.*<sup>4a</sup> on the basis of the temperature dependent PMR shifts of imidazole and 3,5-dimethylimidazole in the presence of  $Ru(CO)(TPP)$  and  $Ru(CO)$  (mesoporphyrin(IX)dimethyl ester). The conclusions from this work were reaffirmed in a subsequent paper<sup>4b</sup>. The failure of coalesced resonances to approximate the average of the slow exchange chemical shifts of the exchanging nuclei cast considerable doubt on the interpretation and the proposed shuttling mechanism. During the course of this work Faller and Sibert<sup>6</sup> demonstrated that the spectral assignments of Tsutsui *et al.*<sup>4</sup> were incorrect and that imidazole exchange was actually intermolecular, not intramolecular. With the correct peak assignments the downfield shifts of resonances with increasing temperature would be expected, and it is not necessary to invoke “wagging” of the imidazole “through several different orientations with respect to the porphyrin ring”<sup>4a</sup>. The peak Tsutsui

*et al.* assigned to coalescence of imidazole protons 4 and 5 appears to be due to coalescence of proton 2 with roughly 6% free ligand. Judging from the report that  $\Delta G^\ddagger = 18.3$  kcal/mol at 64<sup>o</sup>6 and from the results in Table 1, it is likely that spectra at higher temperatures than that reported by Tsutsui *et al.* would be needed to observe coalescence of the signals of imidazole protons 4 and 5 [*e.g.*, *cf.* the spectra of Ru(CO)-(i-Pr-TPP)(t-Bupy)<sup>5</sup>].

Even in the case of 3,5-DMP, which would appear to maximize the opportunity for intramolecular ligand site exchange with concomitant hydrogen migration, no evidence for an intramolecular exchange was found. Further, it was expected that the lowest energy pathway for site exchange would involve two equivalent donor sites. The present study demonstrates that this process does occur with Ru(CO)(i-Pr-TPP)-(4,5-DMPD) and Ru(CO)(i-Pr-TPP)(3,6-DMPD). The low temperature portions of Figs. 4 and 6 reveal coalescence of the methyl signals of the coordinated ligands before the rates of intermolecular ligand exchange appreciably affect the spectra. The PMR results do not allow identification of the detailed pathway for site exchange, and the intermediate or transition state in eqn. (6) is merely the most symmetrical of many which could be proposed.

#### Lability of porphyrin complexes

As noted above, ligand exchange reactions of Ru(CO)(i-Pr-TPP)(L) are unusually fast for complexes containing an Ru<sup>II</sup>-N bond. Facile displacement of axial ligands in metalloporphyrins has ample precedent. Such reactions are well known for vitamin B<sub>12</sub><sup>21</sup> and proceed at rates ca. 10<sup>7</sup> times faster than for the cobaloxime Co(DH)<sub>2</sub>(NO<sub>2</sub>)(H<sub>2</sub>O),<sup>22,23</sup> for example. Anation reactions of Co<sup>III</sup> hematoporphyrin are nearly as fast as for vitamin B<sub>12</sub> derivatives<sup>24</sup>. More recently, Cr<sup>III</sup> tetra-(*p*-sulfonatophenyl)porphine complexes have been shown to undergo substitution reactions about 10<sup>3</sup>-10<sup>4</sup> times faster than normal, substitution-inert, Cr<sup>III</sup> complexes<sup>25</sup>. In view of these results it is perhaps not surprising that the Ru<sup>II</sup> complexes investigated in this work show enhanced kinetic lability compared to more conventional six-coordinate complexes<sup>1</sup>.

In addition, it has been suggested, based on an approximate treatment of the PMR data for Ru(CO)(mesoporphyrin(IX)dimethyl ester)(Py), that the Ru<sup>II</sup> is displaced above the mean N<sub>4</sub> plane of the porphine<sup>4</sup>, as has been found for a number of five coordinate metalloporphyrins<sup>26</sup>. Regardless of the extent of displacement, steric interactions between the porphine and an axial ligand limit the accessibility of Ru<sup>II</sup> to nitrogen donor ligands. Since Taube<sup>1</sup> has considered metal→ligand  $\pi$ -backbonding to contribute appreciably to the stability of complexes such as [Ru(NH<sub>3</sub>)<sub>5</sub>(Py)]<sup>+2</sup>, any suppression of  $\pi$ -backbonding between Ru<sup>II</sup> and the axial ligand due to the effect of the *trans* carbon monoxide could tend to increase the lability of the Ru(CO)-(porphyrin)(L) complexes. Others have invoked  $\pi$ -backbonding effects in rationalizing the stabilities of Fe<sup>II</sup>(porphyrin)(L)<sup>27-29</sup> and small changes in the C-O stretching frequencies of Fe(CO)(porphyrin)(L)<sup>30</sup> complexes. Analogous apparent dependence on  $\pi$ -bonding capability of the axial ligand has been observed with Mg(porphyrin)(L) complexes<sup>31</sup>, and in the iron complexes a strong dependence on the nature of the porphyrin was noted<sup>29</sup>. It has also been pointed out that specific solvation effects and entropy changes may contribute strongly to the observed stabilities of metalloporphyrin complexes<sup>29</sup>.

### Rotation of phenyl groups

In addition to intermolecular ligand and intramolecular site exchange, a third kinetic process has been detected. The PMR spectrum of the free porphine  $H_2(i\text{-Pr-TPP})$  shows that the four phenyl protons are pairwise equivalent at  $25^\circ$  in tetrachloroethane solution. However, under the same conditions  $Ru(CO)(i\text{-Pr-TPP})$  and its base adducts give an  $AA'BB'$  phenyl proton spectrum since the phenyl rings are sterically constrained to be at an angle with respect to the porphine mean plane. The spectra shown in Fig. 9 show that as the temperature is raised the phenyl signals broaden and finally collapse to an AB pattern. Spectral changes are reversible with temperature. The only means by which the two different *o*- and *m*-protons can become equivalent is by rotation about the *meso* carbon-phenyl C-C bond. No attempt was made to obtain accurate kinetic parameters, but an approximate treatment<sup>32</sup> yields ca.  $60 \text{ sec}^{-1}$  as the rate of rotation about the C-C bond at the coalescence temperature of ca.  $95^\circ$ , and  $\Delta G^\ddagger 18.6 \pm 0.5 \text{ kcal/mole}$ . The only other report of bond rotation in porphines concerns tetra(*o*-hydroxyphenyl)porphine,  $H_2(\text{THPP})$ . Isomers of this compound could be separated and the rate constant for rotation at  $23^\circ$  in methanol is  $1.5 \times 10^{-5} \text{ sec}^{-1}$  ( $\Delta G^\ddagger 24 \text{ kcal/mole}$ )<sup>33</sup>. Rotation was about 10 times slower for  $Cu(\text{THPP})(H_2O)$  in aqueous methanol. This difference in rates was interpreted as indicating that  $H_2(\text{THPP})$  must distort considerably in the transition state and that the more rigid  $Cu^{II}$  complex is less susceptible to such distortions. The PMR spectra

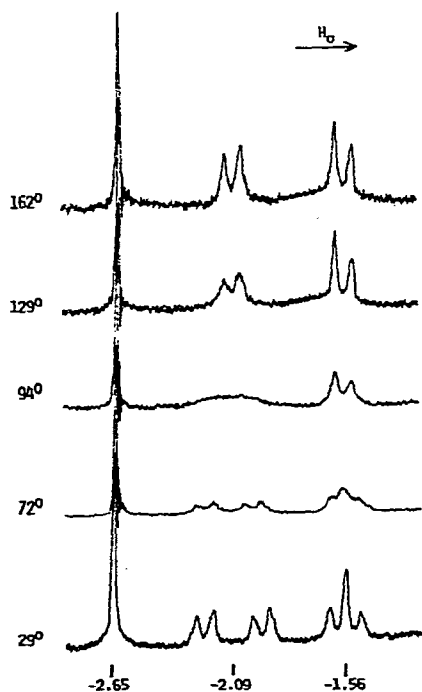


Fig. 9. 100 MHz PMR spectra of the phenyl resonances of  $Ru(CO)(i\text{-Pr-TPP})$  in  $C_2H_2Cl_4$  solution in the presence of excess 4,5-DMPD at various temperatures. Slow exchange chemical shifts are in ppm from the  $C_2H_2Cl_4$  lock signal (negative values denote downfield shifts). The  $-2.65 \text{ ppm}$  resonance is due to the porphine pyrrole protons.



of nickel [tetra(*o*-tolyl)porphine] contain multiple methyl signals which do not appreciably broaden up to 180°, indicating  $\Delta G^\ddagger$  for rotation exceeds 26 kcal/mol<sup>34</sup>. The much more rapid phenyl group rotation in Ru(CO)(*i*-Pr-TPP) reflects the greater steric barrier imposed by *o*-OH or *o*-CH<sub>3</sub> compared to *o*-H.

## ACKNOWLEDGMENT

This research was supported by the National Institutes of Health under grant GM-15471.

## REFERENCES

- 1 P. C. Ford, *Coord. Chem. Rev.*, 5 (1970) 75; H. Taube, in *Survey of Progress in Chemistry*, to be published.
- 2 Sr. H. Elsbernd and J. K. Beattie, *Inorg. Chem.*, 8 (1969) 983.
- 3 J. G. Gordon, II, M. J. O'Connor, and R. H. Holm, *Inorg. Chim. Acta*, 5 (1971) 381.
- 4 a. M. Tsutsui, D. Ostfeld and L. M. Hoffman, *J. Amer. Chem. Soc.*, 93 (1971) 1820.  
b. M. Tsutsui, D. Ostfeld, J. N. Francis, and L. M. Hoffman, *J. Coord. Chem.*, 1 (1971) 115.
- 5 S. S. Eaton, G. R. Eaton, and R. H. Holm, *J. Organometal. Chem.*, 32 (1971) C52.
- 6 J. W. Fallor and J. W. Sibert, *J. Organometal. Chem.*, 31 (1971) C5.
- 7 R. H. Horning and E. D. Amstutz, *J. Org. Chem.*, 20 (1955) 707.
- 8 J. Levisalles, *Bull. Soc. Chim. Fr.*, (1957) 1004.
- 9 C. G. Overberger, N. R. Byrd, and R. B. Mesrobian, *J. Amer. Chem. Soc.*, 78 (1956) 1961.
- 10 A. D. Adler, F. R. Longo, J. D. Finarelli, J. Goldmacher, J. Assour, and L. Korsakoff, *J. Org. Chem.*, 32 (1967) 476.
- 11 J. Krieger, Ph. D. Thesis, M.I.T., 1971.
- 12 G. M. Whitesides and J. S. Fleming, *J. Amer. Chem. Soc.*, 89 (1967) 2855; J. S. Lisle, S. B. Thesis, M.I.T., 1968.
- 13 J. R. Hutchison, J. G. Gordon, II, and R. H. Holm, *Inorg. Chem.*, 10 (1971) 1004.
- 14 J. E. Maskasky and M. E. Kenney, *J. Amer. Chem. Soc.*, 93 (1971) 2060, and references therein.
- 15 S. N. Vinogradov and M. Kilpatrick, *J. Phys. Chem.*, 68 (1964) 181.
- 16 A. Albert, R. Goldacre, and J. Phillips, *J. Chem. Soc.*, (1948) 2240.
- 17 J. Levisalles, *Bull. Soc. Chim. Fr.*, (1957) 1009.
- 18 H. C. Brown and B. Kanner, *J. Amer. Chem. Soc.*, 88 (1966) 986, and references therein.
- 19 C. H. Kirksey, P. Hambright, and C. B. Storm, *Inorg. Chem.*, 8 (1969) 2141.
- 20 C. H. Kirksey and P. Hambright, *Inorg. Chem.*, 9 (1970) 958.
- 21 P. George, D. H. Irvine, and S. G. Glauser, *Ann. N.Y. Acad. Sci.*, 88 (1960) 393.
- 22 W. C. Randall and R. A. Alberty, *Biochemistry*, 5 (1966) 3189; *ibid.*, 6 (1967) 1520.
- 23 D. N. Hague and J. Halpern, *Inorg. Chem.*, 6 (1967) 2059.
- 24 E. B. Fleischer, S. Jacobs and L. Mestichelli, *J. Amer. Chem. Soc.*, 90 (1968) 2527.
- 25 E. B. Fleischer and M. Krishnamurthy, *J. Amer. Chem. Soc.*, 93 (1971) 3784.
- 26 E. B. Fleischer, *Accounts Chem. Res.*, 3 (1970) 105.
- 27 J. E. Falk and J. N. Phillips, in F. P. Dwyer and D. P. Mellow (Ed.), *Chelating Agents and Metal Chelates*, Academic Press, New York, 1964, ch. 10.
- 28 J. J. R. Frausto Da Silva and J. G. Caládo, *J. Inorg. Nucl. Chem.*, 28 (1966) 125.
- 29 S. J. Cole, G. C. Curthoys, and E. A. Magnusson, *J. Amer. Chem. Soc.*, 92 (1970) 2991.
- 30 J. O. Alben and W. S. Caughey, *Biochemistry*, 7 (1968) 175.
- 31 C. B. Storm, A. H. Corwin, R. R. Arellano, M. Martz, and R. Weintraub, *J. Amer. Chem. Soc.*, 88 (1966) 2525.
- 32 J. A. Pople, W. G. Schneider, and H. J. Bernstein, *High-Resolution Nuclear Magnetic Resonance*, McGraw-Hill, New York, 1959, p. 223.
- 33 L. K. Gottwald and E. F. Ullman, *Tetrahedron Lett.*, 36 (1969) 3071.
- 34 F. A. Walker and G. L. Avery, *Tetrahedron Lett.*, 36 (1969) 4949.

*J. Organometal. Chem.*, 39 (1972)